Large flexibility of high aspect ratio carbon nanostructures fabricated by electron-beam-induced deposition

2010 Nanotechnology 21 475702

(http://iopscience.iop.org/0957-4484/21/47/475702)

Nanotechnology **21** (2010) 475702 (4pp) doi:10.1088/0957-4484/21/47/475702

Large flexibility of high aspect ratio carbon nanostructures fabricated by electron-beam-induced deposition

J D Beard and S N Gordeev

Department of Physics, University of Bath, Bath BA2 7AY, UK

E-mail: jdb28@bath.ac.uk

Received 5 July 2010, in final form 15 September 2010
Published 29 October 2010
Online at stacks.iop.org/Nano/21/475702

Abstract
The mechanical properties of free-standing electron beam deposited amorphous carbon structures have been studied using atomic force microscopy. The fabricated carbon blades are found to be extraordinarily flexible, capable of undergoing vertical deflection up to ∼75% of their total length without inelastic deformation. The elastic bending modulus of these structures was calculated to be 28 ± 10 GPa.

(Some figures in this article are in colour only in the electronic version)

1. Introduction

Electron-beam-induced deposition (EBID) is a very versatile, widely applied method allowing the direct fabrication of 2D and 3D nanostructures of many different materials [1–5]. It is capable of high spatial resolution, with sub-nanometre resolution possible [6, 7]. It has the advantage of allowing single-stage nanofabrication, without requiring a mask or chemical processing, and can be performed using a standard unmodified SEM system.

EBID occurs when an energetic electron beam (typically 1–200 kV) is incident on a substrate. Interaction between the incident primary electrons and the substrate atoms produces secondary electrons of energy 1–50 eV, which are able to decompose 'precursor' hydrocarbon molecules present in the vacuum chamber [8]. These molecules are decomposed by the beam, creating a solid deposit on the substrate; typically amorphous carbon, but other materials can be deposited using different precursor substances [2–5]. Control of the beam using an electron beam lithography (EBL) system allows the fabrication of complex structures [1]. EBID has been applied to fabricate a wide variety of nanoscale structures including lithography masks, nanodots, nanowires and contacts [1]. It can also be used for the 'welding' of nano-objects to substrates [9], and for the modification of atomic force microscope (AFM) probes to improve their aspect ratio [10, 11] or suitability for mechanical lithography [12]. Our group recently reported the fabrication of thin blades of amorphous carbon on AFM probes using an EBID technique, and showed how these blades could be applied as 'nanoscalpels' for mechanical lithography on gold films and the dissection of nanoscale biological objects [13]. For many applications, the mechanical properties of the deposited structures become important—they must be resilient enough to withstand the forces applied to them without breaking. However, studies of the mechanical properties of EBID structures have only been carried out on area deposits on flat substrates [14] and not on high aspect ratio free-standing EBID structures.

This paper describes an experiment to measure the mechanical properties of the deposited carbon blades. It was discovered in the course of this experiment that the carbon blades demonstrate surprising flexibility, and are able to recover elastically from large deformations.

2. Experimental details

To fabricate a blade, the 20 keV electron beam of a scanning electron microscope (SEM) was focused on a point ∼100 nm from a substrate edge and then moved beyond the edge at a velocity of 1–10 nm s^{-1} (see figure 1). This method creates a free-standing structure from amorphous carbon [15, 16]. No precursor gas was deliberately introduced into the SEM chamber—as in many other experiments [10–12], EBID was performed using adventitious hydrocarbons already present in standard SEM vacuum systems. The pressure in the SEM

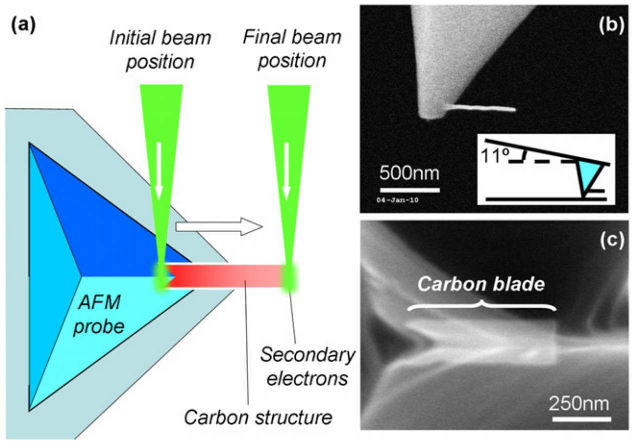

Figure 1. (a) Fabrication process for an amorphous carbon blade by electron-beam-induced deposition. (b) and (c) SEM images of a blade immediately after fabrication, imaged from the edge (b) and top (c). Inset diagram in (b) shows the carbon blade alignment during AFM imaging. SEM images were taken using beam energy of 20 keV, beam current ∼120 pA.

system was measured at 2×10^{-5} mbar; it should be noted that most of the residual gas in the vacuum system is non-carbon-bearing e.g. hydrogen or water vapour and so does not contribute to the deposition.

For mechanical testing, carbon blades of length 450–650 nm, width 150–200 nm, and thickness of ∼40 nm were grown close to the apex of standard tapping mode AFM probes (see figure 1). These probes have a nominal spring constant of ∼40 N m^{-1} and a resonant frequency of ∼300 kHz. The carbon blades were fabricated such that they lie parallel to the plane of the sample surface when the probe is mounted in the AFM system. The probe cantilever spring constant k_c was calculated using $k_c = 0.2425m\omega_0^2$ where ω_0 is the cantilever cyclic resonant frequency and m is the cantilever mass calculated from its density and geometry [17]. Mechanical testing was performed by approaching and retracting the tip onto the surface of a standard AFM calibration grid. This grid consists of an array of well-defined 5 μm × 5 μm microfabricated pits with a depth of 200 nm. Approach–retract curves were recorded close to a 200 nm step on the sample surface, such that the carbon blade is deflected before the more rigid silicon AFM tip can come into contact with the sample surface (see figure 2(a)). The deflection of the carbon blade is then measurable from this force curve by comparison to a 'reference curve' recorded on a flat area of the sample where only the silicon tip (and not the carbon blade) comes into contact with the surface.

3. Results

The mechanical properties of the carbon blades can be determined by examination of the approach–retract curves obtained during the AFM measurements. During the initial stage of the approach, no deflection is detected as the carbon blade is not in contact with the surface (region (i) in figure 2(b)). As the carbon blade makes contact with

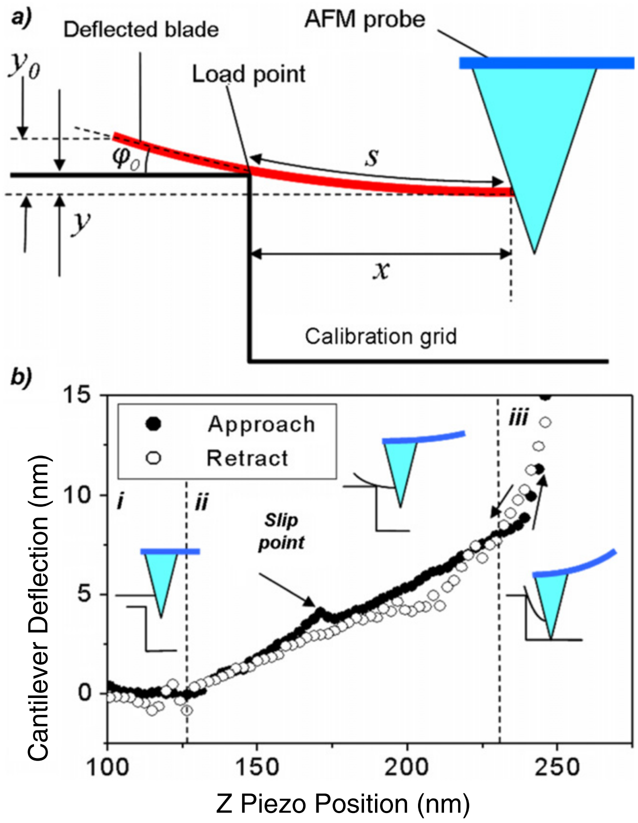

Figure 2. (a) Experimental setup. The carbon blade is deflected against a 200 nm step during an approach–retract cycle of the AFM probe. (b) A typical force curve, showing different interaction regimes of the probe and carbon blade with the step. The approach and retract curves show little or no hysteresis, indicating that the carbon blade is deformed elastically. The inset diagrams show the deflection of the carbon blade against the step.

the step, the force applied to the blade is detected as a small linear increase in cantilever deflection (region (ii)). In many approach/retract curves, an abrupt change in gradient is observed while the carbon blade deflects. This can be attributed to rapid 'slipping' of the carbon blade down the step, causing a sudden change in the load point position. Finally, in region (iii) a rapid increase in deflection is observed as the silicon tip itself comes into contact with the sample surface. Little or no hysteresis is visible in the force curves, even for large deformations, indicating that the carbon blades are deformed elastically. The deflection of the carbon blade is then measured from region (ii) of the force curve. The spring constant, k, of the blade can then be calculated from the deflection of the carbon blade as a function of the applied force.

In order to calculate the deflection, y_0, angle of the carbon blade to the horizontal at the load point, φ_0, and bending modulus E for the carbon blade, it is necessary to describe the bending of the blade using the widely applied Euler–Bernoulli beam equation [18]. This equation is $EI(\mathrm{d}\varphi/\mathrm{d}s) = M$ where E is the 'elastic bending modulus' of the blade, I is its 'second moment of inertia' equal to $I = wt^3/12$ for a beam of rectangular cross-section of width and thickness $w \times t$, $\mathrm{d}\varphi/\mathrm{d}s$ is the curvature of the beam, and M is the bending moment. This equation is fundamental to the prediction of

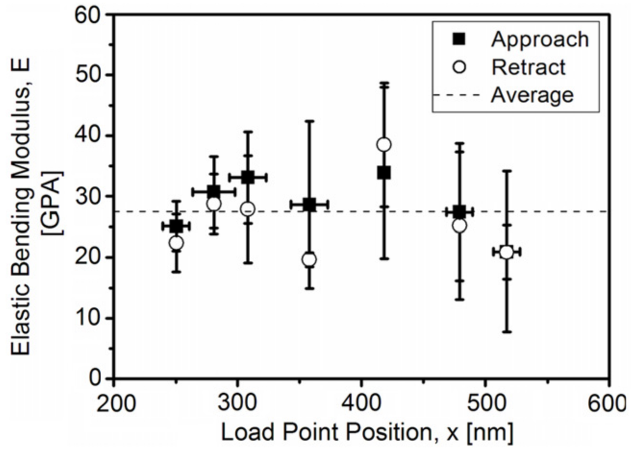

Figure 3. Elastic moduli of a carbon blade calculated using the numerical model from experimental AFM curves, as a function of the load position. Error bars indicate the spread of calculated values from separate force curves recorded on the same carbon blade.

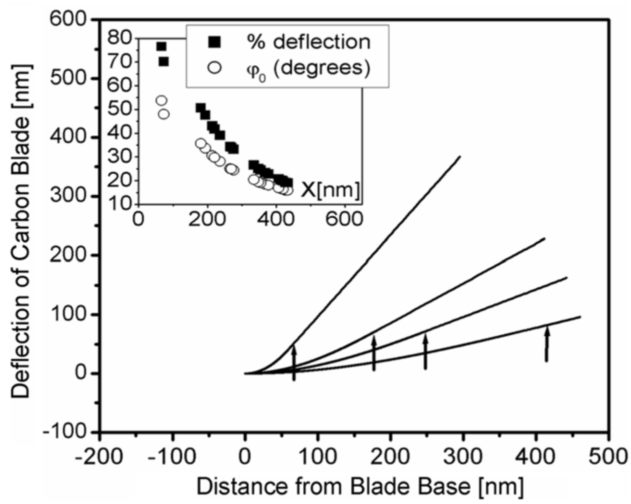

Figure 4. Calculated shapes of deflected carbon blades for different load point positions (arrowed). Inset shows deflection of the free end of the carbon blade as a percentage of its total length (y_0/L) and its angle of deflection φ_0, as a function of the load position x.

the behaviour of beam-like components in engineering, and is often applied to microscale or nanoscale objects including AFM cantilevers [19]. For deflections larger than ~5% of the total beam length, the Euler–Bernoulli equation requires numerical computation to solve, using a model proposed by Bisshop and Drucker [20–22]. Using this model we calculated a bending modulus of 28 ± 10 GPa for the carbon blades (see figure 3).

4. Discussion

A previous study by Ding *et al* using an AFM-based nanoindentation technique on areal deposits of EBID carbon reported an elastic modulus ranging from ~34 GPa for deposition using 3 keV electrons to 60 GPa for 20 keV [14]. The properties of amorphous carbon depend strongly on the proportion of sp^2 to sp^3 bonds within the material [23], and these vary with the type of precursor used, electron beam energy and other experimental conditions. Ding *et al* found that their carbon deposits consisted of 83% sp^2 bonded carbon. The lower elastic modulus determined for our carbon structures suggests that they have a higher sp^2 content, which tends to decrease the elastic modulus of amorphous carbon [23]. This could be attributed to the different growth conditions used to grow free-standing structures in our experiment, as opposed to the growth of areal structures on substrates in previous studies [14]. In particular, the length of time over which the structure is exposed to the primary (high-energy) electron beam is much shorter in our experiment.

The Bisshop–Drucker model also allows calculation of the shape of the deflected carbon blade. Examples of deflected blade shapes are shown in figure 4. This calculation showed that in our experiment the blades were deformed such that the free end was deflected up to >75% of the total blade length, with a radius of curvature <100 nm, without breaking or undergoing detectable inelastic deformation, even after repeated deflection and relaxation. The calculated deflection of the beam is shown graphically in the inset in figure 4. The large elastic deformation of these blades is a striking result suggesting extreme elasticity and flexibility of the deposited material. This also suggests that the blades are highly amorphous with little or no brittle crystalline structure.

The high flexibility and elastic response of these blades suggests that they may have many potential nanotechnological applications. They could be employed as nanoscale springs, electromechanical oscillators or force transducers. They could also be applied as nanocantilever chemical sensors or biosensors, which function by detecting a change in the resonance or deflection of a flexible cantilever due to the binding of molecules to the cantilever [24]. Nanocantilever sensors demonstrate high specificity and sensitivity, with single-molecule detection possible [25]. The EBID fabrication process allows the creation of free-standing nanoscale structures without the complex multistage processes which are usually used in the fabrication of such devices. In our experiments we have been able to grow carbon blades with thicknesses ranging from 20 to 60 nm, with lengths from 200 to 750 nm. In experiments by other groups using higher-energy electron beams, EBID of free-standing structures with a thickness of ~10 nm has been demonstrated [26]. This would suggest that the spring constant of these carbon blades could range from 10^{-4} to ~10 N m^{-1} with resonant frequencies of 0.01–1 GHz. Using shorter blades or further decreasing their thickness would further expand the range of frequencies and spring constants attainable, allowing 'tuning' of these properties for different applications.

5. Conclusions

In summary, we have been able to measure the bending modulus of free-standing amorphous carbon structures fabricated by EBID. We have found that the blade-like structures created can be repeatedly deflected up to ~75% of their total length without inelastic deformation. The elastic bending modulus of these blades was determined using a numerical calculation based on the experimental results, and was found to be 28 ± 10 GPa.

References

[1] Randolph S J, Fowlkes J D and Rack P D 2006 *CRC Crit. Rev. Solid State Mater. Sci.* **31** 55

[2] Gazzadi G C, Frabboni S and Menozzi C 2007 *Nanotechnology* **18** 445709

[3] Botman A, Mulders J J L, Weemaes R and Mentink S 2006 *Nanotechnology* **17** 3779

[4] Cho C C and Bernasek S L 1989 *J. Appl. Phys.* **65** 3035

[5] Cicoira F, Leifer K, Hoffmann P, Utke I, Dwir B, Laub D, Buffat P A, Kapon E and Doppelt P 2004 *J. Cryst. Growth* **265** 619

[6] van Dorp W F, van Someren B, Hagen C W and Kruit P 2005 *Nano Lett.* **5** 1303

[7] Hagen C Q, Silvis-Cividjian N and Kruit P 2006 *Scanning* **28** 204

[8] Ennos E A 1953 *Br. J. Appl. Phys.* **4** 101

[9] Burbridge D J, Crampin S, Viau G and Gordeev S N 2008 *Nanotechnology* **19** 445302

[10] Schiffmann K I 1993 *Nanotechnology* **4** 163

[11] Chen I-C, Chen L-H, Orme C, Quist A, Lal R and Jin S 2006 *Nanotechnology* **17** 4322

[12] Wendel M, Lorenz H and Kotthaus J P 1995 *Appl. Phys. Lett.* **67** 3732

[13] Beard J D, Burbridge D J, Moskalenko A V, Dudko O, Yarova P L, Smirnov S V and Gordeev S N 2009 *Nanotechnology* **20** 445302

[14] Ding W, Dikin D A, Chen X, Piner R D, Ruoff R S, Zussmann E, Wang X and Li X 2005 *J. Appl. Phys.* **98** 014905

[15] Kreuzer P 1998 *Optik* **78** 158
Möllenstedt G 1988 *Optik* **78** 132

[16] Kislov N A, Khodos I I, Ivanov E D and Barthel J 1996 *Scanning* **18** 114

[17] Sader J E, Chon J W M and Mulvaney P 1999 *Rev. Sci. Instrum.* **70** 3867

[18] Gere J M and Timoshenko S P 1999 *Mechanics of Materials* 4th edn (Cheltenham: Stanley Thornes)

[19] Sarid D 1991 *Scanning Force Microscopy with Applications to Electric Magnetic and Atomic Forces* (New York: Oxford University Press)

[20] Bisshopp K E and Drucker D C 1945 *Q. Appl. Math.* **3** 272

[21] Belendez T, Neipp C and Belendez A 2002 *Eur. J. Phys.* **23** 371

[22] Ding W, Guo Z and Ruoff R S 2007 *J. Appl. Phys.* **101** 034316

[23] Marques F C, Lacerda R G, Champi A, Stolojan V, Cox D C and Silva S R P 2003 *Appl. Phys. Lett.* **83** 3099

[24] Lavrik N V, Sepaniak M J and Datskos P G 2004 *Rev. Sci. Instrum.* **75** 2229

[25] Lavrik N V and Datskos P G 2003 *Appl. Phys. Lett.* **82** 2697

[26] Lui Z Q, Mitsuishi K and Furuya K 2005 *Appl. Phys.* A **80** 1437